Research Square

Preprints are preliminary reports that have not undergone peer review.
They should not be considered conclusive, used to inform clinical practice,
or referenced by the media as validated information.

Targeted siRNA-Lactobionic Lipid Nanoparticles with Novel Ionizable Lipid Inhibit Antithrombin III Expression in Hepatocytes

Ali Rajabi Zangi
Tabriz University of Medical Sciences
Seyed Hossein Kiaie
Alborz University of Medical Sciences
Seyed Milad Safar Sajadi
University of Tehran
Hamid Reza Heidari
Tabriz University of Medical Sciences
Hamed Hamishehkar
Tabriz University of Medical Sciences
Yousef Javadzadeh
javadzadehy@yahoo.com

Tabriz University of Medical Sciences

Research Article

Keywords: Hemophilia, lipidNanoParticles, AntiThrombinIII, Drug Delivery, Hepatocyte, siRNA

Posted Date: June 29th, 2026

DOI: https://doi.org/10.21203/rs.3.rs-10038643/v1

License: This work is licensed under a Creative Commons Attribution 4.0 International License.
Read Full License

Additional Declarations: No competing interests reported.

Abstract

Targeted reduction of hepatic antithrombin (AT) via siRNA offers a promising strategy to enhance thrombin (TMB) generation in bleeding disorders, though efficient hepatocyte delivery remains challenging. This study developed and evaluated a targeted lipid nanoparticle (LNP) formulation incorporating a novel morpholine-based ionizable lipid (MIL) and a lactobionic-octadecylamine conjugate (LBN) for hepatocyte-specific delivery of AT-siRNA (siAT). Following synthesis of MIL and LBN, siAT-loaded LNPs (siAT LNP LBN) were prepared using microfluidics and characterized for size, morphology, zeta potential, polydispersity index, and encapsulation efficiency (EE). Functional assays on HepG2 cells assessed cellular uptake, protein knockdown, and AT activity. The optimized formulation exhibited uniform particles (124 nm, PDI 0.125, zeta potential − 8.9 mV) and high EE (90%). Cytotoxicity assays confirmed safety up to 65 pmol siRNA. LBN-decorated LNPs significantly enhanced hepatocyte uptake compared to non-targeted LNPs and naked siRNA. Optimal AT mRNA suppression occurred at ~ 65 pmol siRNA and 16 h, with protein knockdown confirmed at 48 h. Functionally, siAT LNP LBN reduced AT activity to 4.1%, substantially outperforming non-targeted LNP (64.1%) and naked siRNA (86.6%). The developed siAT LNP LBN platform enables efficient hepatocyte delivery, achieving robust AT knockdown and low cytotoxicity, warranting further in vivo evaluation for bleeding disorder management.

1. Introduction

Hemophilia (HMP) is a group of inherited bleeding disorders, primarily Hemophilia A (deficiency of factor VIII, FVIII) and Hemophilia B (deficiency of factor IX, FIX), that cause impaired hemostasis and recurrent bleeding into joints and muscles, leading to chronic arthropathy, disability, reduced quality of life, and increased health-care burden. Thrombin (TMB) amplifies coagulation by activating cofactors (FV, FVIII) and antithrombin (ATB) blocks TMB and other activated coagulation factors (e.g., FXa). The hemostatic balance depends on adequate TMB generation for clot formation and sufficient anticoagulant control to prevent thrombosis. In hemophilia, insufficient upstream cofactor activity (FVIII or FIX) leads to inadequate TMB generation and bleeding[1, 2].

Advanced therapies (factor replacement, prolonged half-life factors, and non-factor agents) have markedly improved outcomes, but access, cost, and inhibitor development (neutralizing antibodies) remain major challenges worldwide[3, 4]. Inhibiting ATB can enhance TMB generation by reducing the principal physiological brake on the coagulation cascade, thereby partially compensating for deficits in FVIII or FIX [2, 5].

ATB activity can be suppressed through antisense oligonucleotides (ASOs) or small interfering RNA (siRNA), which reduce ATB synthesis in the liver; monoclonal antibodies or engineered proteins that neutralize ATB; and small molecule inhibitors. Among these, siRNA platforms offer an inspiring solution, given that the liver is the primary site of ATB production and hepatic gene silencing effectively reduces ATB levels. Fitusiran, an siRNA therapeutic that lowers ATB to boost TMB generation in people with hemophilia, has demonstrated improved bleed control but has also produced thrombosis signals at high

levels of ATB suppression, underscoring the need for controlled dosing and proactive risk-mitigation strategies [6–8]. Fitusiran is designed for hepatocyte-targeted delivery by conjugating it to N-acetylgalactosamine (GalNAc) ligands. These GalNAc moieties bind with high affinity to the asialoglycoprotein receptor (ASGPR), which is predominantly expressed on hepatocyte surfaces [9, 10].

The siRNA platform offers highly specific, long-lasting protein knockdown with infrequent dosing and is well-suited for liver targets. Major challenges include off-target effects, immune activation, variable and sometimes inefficient hepatocyte delivery, interpatient variability, and a narrow therapeutic window. Excessive ATB suppression can cause thrombosis, raising concerns about long-term safety, reversibility, and managing breakthrough thrombosis[11] .

Lipid nanoparticles (LNPs) enhance siRNA stability, promote intracellular delivery, and improve cytoplasmic release following endosomal trafficking, typically contain ionizable lipids (ILs), DSPC, cholesterol, and PEG-lipids. For active targeting, ligands such as GalNAcand other sugar moieties have been used to engage ASGPR for targeted uptake[12, 13]. Lactobionic acid (LBA), a galactose-containing ligand, can similarly bind hepatic lectin receptors and has been explored as a targeting ligand to enhance hepatocyte specificity. Conjugating ligands to LNP surfaces or to siRNA can enhance delivery efficiency and allow lower doses[14, 15].

Targeted siRNA-Lactobionic LNP is a necessary strategy for ATB inhibition because it enables potent, durable, and hepatocyte-specific knockdown of ATB expression while minimizing off-target effects and systemic toxicity: siRNA molecules designed against the SERPINC1 transcript can harness the RNA-induced silencing complex to selectively reduce hepatic ATB synthesis, and LNP optimized for liver delivery protect siRNA from nuclease degradation, promote efficient endosomal escape, and permit controlled dosing to achieve clinically relevant reductions in plasma ATB that rebalance coagulation in bleeding disorders for hemophilia that reduces plasma ATB levels, underscoring the therapeutic potential and necessity of targeted siRNA-LNP platforms for safe and effective ATB inhibition [16]. In this study, the novel IL and targeted ligand, a conjugation of LBA to an amine moiety (LBN), were synthesized. Then, a unique LNP formulation that included IL and LBN was developed to effectively and target-deliver siRNA to HepG2 cell lines. The Targeted siRNA-LNP decreases the mRNA expression and protein levels of AT III in hepatocyte cells.

2. Materials and methods

2.1. Materials

The lauryl acrylate (LA), 4-(2-Aminoethyl)morpholine (AEM), lactobionic acid (LBA), and octadecylamine were supplied by Sigma-Aldrich (Germany). 1,2-distearoyl-sn-glycero-3-phosphocholine (DSPC), cholesterol, and 1,2-dimyristoyl-rac-glycero-3-methoxypolyethylene glycol-2000 (DMG-PEG2000) were provided by Avanti Polar Lipids, Inc.. Silica gel 60 (230–400 mesh, Merck) was used as the stationary phase for column chromatography. Lipofectamine 2000 was acquired from Invitrogen (Grand Island,

New York), while 3-(4, 5-dimethylthiazol-2-yl)-2, 5-diphenyl tetrazolium bromide (MTT) and Triton X-100 were purchased from Sigma Aldrich (St. Louis, Missouri). The siRNA was labeled with FITC, siAT(FITC) for targeting ATB (mouse) was supplied by Santa Cruz Biotechnology (Uppsala, Sweden), and the primers were purchased from BioLegend (Uppsala, Sweden). HEPG2 cells were kindly supplied by the Immunology Research Center, Tabriz, Iran.

2.2.Methods

2.2.1. Preparation and structural analysis of ionizable lipid and targeted moiety

The morpholine-based IL (MIL) was synthesized using reaction of AEM (0.1 g) and freshly distilled LA (0.492 g) under 80°C, a N_2 atmosphere and light protection for 48 h. Purification of the crude product was checked using silica gel column chromatography with DCM/MeOH/NH_4OH solvent gradient (100:0:0 to 100:10:1) and reaction development was visualized by thin-layer chromatography (TLC). Following concentration of the selected fractions under reduced pressure (rotary evaporation), 0.46 g viscous oil product (MIL) (Fig. 1) was synthesized (98% yield)and stored at -20°C under N_2 atmosphere.

To synthesize the targeted moiety (LBN), a solution of LBA (0.985 g, 0.27 mmol) and octadecylamine (1.00 g, 0.37 mmol) in dimethyl sulfoxide (DMSO) (15 mL) was first prepared. Subsequently, 1-ethyl-3-(3-dimethylaminopropyl)carbodiimide (EDC; 0.65 g), 4 (dimethylamino)pyridine (DMAP) (65 mg), and triethylamine (Et3N) (five drops) were added at RT. The reaction was carried out at 60°C for 24 h under nitrogen atmosphere. Then, the mixture was added dropwise to cold acetone (150 mL) and further washed with an additional portion of cold acetone (50 mL). The precipitate was collected by filtration and dried under vacuum using a rotary evaporator, affording the product as a cream-colored solid.

To analysis of MIL and LBN chemical structures, Fourier-transform infrared (FT-IR) spectroscopy (Shimadzu 8101M, Kyoto, Japan) and proton nuclear magnetic resonance (^{1}H-NMR) spectroscopy (Bruker AVANCE III 300) were used [17, 18].

2.2.2. Development and characterization of siAT-LNP-LBN

A lipid mixture solution (10 mM) including MIL, cholesterol, DSPC, and DMG-PEG in absolute ethanol at formulated with relative molar proportions of 50:38.5:10:1.5 (x), was prepared (x = LBN). The siRNA targeting AT (siAT), diluted in citrate buffer, and the lipid mixture were combined using a microfluidic device with a nitrogen-to-phosphate (N/P) ratio of 6. The resulting siAT-loaded LNPs containing LBN (siAT-LNP-LBN) were dialyzed overnight against acetate-Tris buffer (pH 7.4) using a PUR-A-Lyzer Maxi 12000 Dialysis kit. Then, the formulation was concentrated to the desired concentration using a 100 kDa Amicon® Ultra centrifugal filter. The final siAT-LNP-LBN formulation was aliquoted into vials and stored at -20°C.

The particle size, polydispersity index (PDI), and zeta potential (ZP) of the targeted nanoparticles were evaluated by dynamic light scattering (DLS) (Malvern Zetasizer, UK) and the morphology of siAT-LNP-LBN was characterized by transmission electron microscopy (TEM) [19, 20].

The encapsulation efficiency (EE)% of siAT-LNPs was assessed using the Quant iT™ RiboGreen (QRG) assay (Invitrogen) and a Hybrid Multi-Mode Microplate Reader (Synergy™, BioTek, USA), according to the company's instructions. In brief, siAT-LNP-LBN samples were incubated at 37°C either in the absence or presence of 1% Triton X-100. After incubation, an RNA detection reagent was introduced into the samples. Fluorescence intensity (FI) measurements were performed at λ_ex = 480 nm and λ_em = 520 nm. The fluorescence signal acquired from samples incubated in the absence of Triton X-100 reflected the total siAT content, whereas the signal from Triton X-100–treated samples corresponded to the unencapsulated (free) siRNA fraction [21].

2.2.3. Cell cultivation and transfection

The human hepatocellular carcinoma-derived HepG2 cells were grown in RPMI-1640 supplemented with 10% FBS and 1% penicillin–streptomycin under controlled conditions (37°C, 5% CO_2, humidified atmosphere). The cells were seeded in T25 flasks (2×10^4 cells per flask) and incubated until 60–70% confluence (24 h) and for cellular uptake studies, HepG2 cells were inoculated into 12-well culture plates (1.1×10^5 cells per well) and incubated overnight to allow cell attachment. Subsequently, the cells were transfected with the following treatments: naked FITC-labeled siAT (FITC-siAT), siAT-loaded LNP (siAT-LNP), and siAT-LNP incorporating LBN (siAT-LNP-LBN). Finally, the cells were maintained in 500 µL of culture medium per well under standard incubation conditions [22].

2.2.4. RNA extraction and RT-PCR

HepG2 cells were exposed to varying concentrations of FITC-labeled siAT-loaded LNP (siAT(FITC)-LNP) and siAT(FITC)-LNP incorporating LBN (siAT(FITC)-LNP-LBN), with Lipofectamine serving as a control. Following 24 h of incubation, 2.2×10^5 cells were harvested and centrifuged at 300 × g for 5 min at 4°C. After cell lysis, RNA purification, RNA extraction, and complementary DNA (cDNA) synthesize (Yekta-Tajhiz kit, Tehran, Iran), the resulting total RNA was eluted and reverse-transcribed into cDNA via PCR amplification carried out at 37°C for 60 min, followed by a 5-min incubation at 70°C. The primer sequences for mouse target genes and the internal control (housekeeping gene) β-actin are presented in Table 1.

Quantitative reverse transcription polymerase chain reaction (qRT-PCR) was executed using SYBR Green chemistry on an Applied Biosystems™ StepOnePlus system with the following thermocycling profile: initial denaturation at 95°C for 15 min; 40 cycles of denaturation at 95°C for 15 Sec. and annealing/extension at 60°C for 1 min; followed by a melting curve analysis consisting of 95°C for 15 Sec, 60°C for 15 Sec, and 95°C for 15 Sec. After incubation, an RNA detection reagent was introduced to the samples. Fluorescence intensity (FI) was recorded at excitation/emission wavelengths of 480/520 nm. Samples without Triton X-100 reflected total siAT content, while Triton X-100–treated samples indicated the fraction of unencapsulated (free) siRNA[23, 24].

Table 1
Sequences of the primers for ATB and β-actin.

Name	Sequence (5’-3’)
ATB	F: GAGACCTACCAGGACATCAGTG
	R: CCTTCGGTCTTATTGGACACCC
β-actin	F: CTGAGCTGCGTTTTACACCCT
	R: TGCTGTCGCCTTCACCGTTC

2.2.5. Cytotoxicity analysis

HepG2 cells were plated in 96-well plates (5.1 × 10^4 cells per well) and administered with either transfected formulations, empty LNP-LBN and of siAT-LNP-LBN (65–85 pmol). Following treatment, Cells were incubated over 24- and 48-hour periods (37°C and 5% CO_2 atmosphere). The culture medium was renewed with fresh medium containing 10% fetal bovine serum (FBS) and 0.5 mg/mL of 3-(4,5-dimethylthiazol-2-yl)-2,5-diphenyltetrazolium bromide (MTT). Following a 4-h incubation (37°C and 5% CO_2), the medium was removed, and 200 µL of dimethyl sulfoxide (DMSO) was applied to each well. The plates were then placed on a shaker and agitated for 30 min under dark conditions to dissolve the formazan crystals. Absorbance at 570 nm (with a reference wavelength of 690 nm) was measured using a Hybrid Microplate Reader (Synergy™, BioTek, USA). Cell viability was calculated relative to control cells using GraphPad Prism version 10 (GraphPad Software, USA) [25, 26].

2.3. Optimization and functional assays

2.3.1. Optimization of dose and exposure time

To determine the optimal concentration (65 to 85 pmol) and exposure time 8 and 48 h post-transfection) for the formulated siAT-LNP-LBN, RT-PCR analysis was utilized. First, HepG2 cells were seeded (2.2 × 10^5 cells per well) in 4-well plates. Following transfection with siAT-LNP-LBN, total RNA was extracted from each well, and cDNA was synthesized via PCR. RT-PCR analysis was conducted to quantify the degree of target gene suppression in each experimental group, enabling quantification of relative gene expression levels. Quantification of messenger RNA (mRNA) expression levels was performed in triplicate by qRT-PCR using RealQ Plus 2x Master Mix Green, High ROX™ (Ampliqon, Denmark) and the corresponding primers [27, 28].

2.3.2. Protein extraction and quantification

Two closely optimized concentrations of siAT-LNP-LBN were evaluated via Western blotting. HepG2 cells were cultured and exposed to an untreated control, naked siAT, siAT-LNP, and siAT-LNP-LBN, all of which were compared relative to the control group. Following 48 h of treatment, Cellular total protein was isolated with RIPA lysis buffer containing a protease inhibitor cocktail, followed by quantification using the bicinchoninic acid (BCA) assay (Thermo Fisher Scientific, USA). Equal amounts of protein (25 µg per

lane) were separated by 10% SDS-PAGE and then transferred onto polyvinylidene difluoride (PVDF) membranes. Membranes were blocked for 1 h at RT with 5% (w/v) non-fat dry milk dissolved in Tris-buffered saline containing 0.1% (v/v) Tween® 20 (TBST). Thereafter, membranes were incubated overnight at 4°C with a primary antibody specific for ATB (dilution 1:1000; Abcam, USA). After thorough washing with TBST, the membranes were incubated with a horseradish peroxidase (HRP)-conjugated secondary antibody (dilution 1:5000; Abcam, USA) for 1 h at RT. Detection of protein bands was performed using ECL reagents and imaged with a gel documentation system. Band intensities were quantified using ImageJ software (National Institutes of Health, USA) and normalized to the corresponding β-actin signal [29, 30].

2.3.3. Flow cytometry analysis

Cellular uptake of FITC-labeled siAT(FITC)-LNP specifically siAT(FITC)-LNP and siAT(FITC)-LNP-LBN was evaluated by flow cytometry with a final siRNA concentration of 65 pmol. HepG2 cells were seeded (5×10^5 cells per well in 6-well) plates and maintained for 24 h under standard culture conditions to ensure attachment (37°C, 5% CO_2). Thereafter, the cells were transfected with either siAT(FITC)-LNP or siAT(FITC)-LNP-LBN and incubated for 12 h.

After completion of the 12-h incubation period, the medium was removed and cells were trypsinized with 0.25% trypsin–EDTA .After cell resuspention with 1 mL of fluorescence-activated cell sorting (FACS) buffer (phosphate-buffered saline (PBS) containing 1% bovine serum albumin (BSA) and 0.1% sodium azide and and maintenance on ice, the cell suspension was centrifuged at 1,500 rpm for 5 min at 4°C and collected. Cells were gently washed twice using ice-cold PBS and centrifugation step at 1,200 rpm for 5 min at 4°C to remove any unbound siRNA. FI was measured using a Partec Cyflow flow cytometer (Partec GmbH, Münster, Germany) equipped with a 488 nm argon-ion excitation laser and a 560 nm long-pass emission filter (FITC channel). FlowJo software was employed for data analysis (version 7.6.1). Cellular uptake efficiency was reported as a percentage of FITC-positive cells relative to the total cell population [31, 32].

2.3.4.Chromogenic assay

ATB activity was measured in citrated plasma using a chromogenic serine protease inhibition assay that quantifies the plasma's ability to neutralize a fixed amount of TMB or factor Xa. Therefore, the samples were diluted in heparin-containing buffer to promote ATB-protease complex formation, incubated with protease, and then reacted with a chromogenic substrate to measure residual enzyme activity spectrophotometrically. Activity was determined by interpolation from a multi-point calibration curve (normal pooled plasma or international standard), and samples were run in replicates alongside calibrators and quality controls[33, 34].

2.4. Data analysis

One-way analysis of variance (ANOVA) was used to compare treatment groups with the control for both qRT-PCR and Western blot data; P values < 0.05 were regarded as statistically significant, and Each assay

was carried out in triplicate with results reported as mean ± standard error [35].

3. Findings and Discussion

3.1. Synthesis and purification of MIL and LBN

A mixture of AEM(0.1 g) and freshly distilled LA (0.492 g) was warmed to 80°C in a nitrogen atmosphere and under dark conditions for 48 h. Silica gel column chromatography was used to purify the crude product employing a DCM/MeOH/NH_4OH gradient (100:0:0–100:10:1). The purification process was monitored by thin-layer chromatography (TLC). Following the solvent removal, the oily product was stored at -20°C under a nitrogen atmosphere, yielding 0.46 g (98%). The synthesis reaction route of the MIL was illustrated in Fig. 1.

To synthesize LBN, a blend of LBA (0.985 g, 0.27 mmol) and Octadecylamine (1.00 g, 0.37 mmol) was dissolved in 15 mL of dimethyl sulfoxide (DMSO). Then, 0.65 g of EDC, 65 mg of DMAP, and 5 drops of Et3N were introduced into the solution at RT. The mixture was heated at 60°C for 24 h under an inert atmosphere. After cooling to RT, the reaction mixture was poured dropwise into 150 mL of cold acetone and washed with an additional 50 mL of cold acetone. Finally, The precipitate was separated and vacuum dried to obtain the product in cream-colored solid form. The synthesis reaction route of the LBN was depicted in Fig. 2.

3.2. Structural analysis using FT-IR evaluation

To confirm the structural integrity of the synthesized MIL and LBN products,FT-IR spectroscopy was performed. The FT-IR spectrum of MIL revealed a medium absorption band at approximately 3279 cm^{-1}, attributed to the N–H stretching vibration (v(N–H)) of the secondary amine. A medium peak in the region of 1580–1650 cm^{-1} corresponds to N–H bending vibrations. A distinct peak observed at 1446 cm^{-1} is assigned to C–H bending. A medium band associated with coupled C–C and C–N stretching vibrations (v(C–C) + v(C–N)) appears between 1450 and 1550 cm^{-1}. Furthermore, peaks at 1330 cm^{-1} and 1460 cm^{-1} are attributed to bending vibrations of CH_2 and CH_3 groups, respectively (Fig. 3)[36].

FT-IR spectroscopy verified the successful conjugation of LBN (Fig. 4). The disappearance of the characteristic carboxylic acid C = O stretching band of the free lipoic acid precursor at approximately 1710 cm^{-1}, coupled with the emergence of amide I and amide II bands at approximately 1629 cm^{-1} and 1541 cm^{-1}, respectively, provides clear evidence of amide bond formation. A broad absorption signal was detected at approximately 3381 cm^{-1} is attributed to O–H stretching vibrations of the carbohydrate moiety of LBN, overlapping with N–H stretching vibrations of the amide group. The intense bands observed at 2920–2851 cm^{-1} correspond to asymmetric and symmetric stretching of aliphatic CH_2 functionalities, confirming the presence of the long C18 alkyl chain derived from octadecylamine. Additionally, the characteristic CH_2 rocking band observed at approximately 719 cm^{-1} further supports the incorporation of the octadecylamine chain. Bands appearing in the 1051–952 cm^{-1} region are

assigned to C–O stretching vibrations of the sugar structure, indicating that the lipoic acid backbone remains intact following conjugation (Fig. 4).

3.3. Structural analysis using NMR analysis

To confirm the structural analysis of the MIL, and LBN products, NMR analysis was done and their ^{1}H-NMR spectra were depicted in Fig. 5.

In the ¹H-NMR spectrum, the signals observed at 0.93 ppm and 1.33 ppm correspond, respectively, to terminal methyl groups (–CH_3, triplet, q) and methylene groups (–CH_2–, h–p) originating from the fatty acid chains. The resonance at 1.66 ppm is attributed to the protons bonded to carbon g, specifically the –COO–CH_2–CH_2– moiety, which appears as a pentet. The signal at 4.08 ppm, a triplet, arises from protons attached to carbon f (–COO–CH_2–). The resonance at 2.48 ppm is assigned to the α-proton (carbon e, –CH_2–COO–CH_2–) adjacent to the ester linkage. Furthermore, signals at 2.26 ppm (singlet), 2.46 ppm (multiplet), and 2.61 ppm (multiplet) are associated with the protons of –CH_3 and –CH_2– groups within the Tris-amine unit. Additionally, the β-proton (carbon d, triplet) adjacent to the ester functionality, corresponding to the –CH_2–CH_2–COO– fragment, appears overlapped at 2.46 ppm (multiplet). The unambiguous assignments of the ¹H-NMR spectra for MIL and LBN are illustrated in Figs. 5 and 6, respectively [37].

3.4. Physicochemical Characterization, Encapsulation Efficiency, and Morphological Analysis of siAT-LNPs

The physicochemical characterization of the LNPs was performed using dynamic light scattering (DLS), revealing a Z-average diameter of 124.1 nm, a zeta potential (ZP) of − 8.8 mV, and a polydispersity index (PDI) of 0.125. Furthermore, transmission electron microscopy (TEM) analysis confirmed the spherical morphology and uniform size distribution of the nanoparticles (Fig. 7).

Moreover, the EE% of siATLNP-LBN was evaluated using the QRG Kit assay (Table 2). Total or encapsulated siRNA concentration and EE% were 109.67 µg/mL and 90.11%, respectively.

Table 2
The summary of the Ribogreen and DLS results.

Ribo Green result			**DLS result**		
EE (%)	Total siAT (µg/mL)	Encapsulated siAT (µg/mL)	Z-Average	ZP (mV)	PDI
82.17	109.67	90.11	124.1	-8.88	0.125

3.5. MTT assay

As shown in Fig. 8, *in vitro* cytotoxicity testing demonstrated that siAT-LNP-LBN containing MIL and LBN produced no significant reduction in HepG2 viability up to 65 pmol compared with the untreated control.

Statistical analysis indicated that siAT-LNP-LBN induced significantly greater cytotoxicity than siAT with less than 70 pmol ($P < 0.05$), indicating that the observed cell death is attributable to the dose-dependent siAT. Experiments were carried out in triplicate, and results are reported as mean ± SD (n = 3).

3.6. Optimization of siRNA Concentration and Incubation Time

Quantitative RT-PCR was conducted to identify the optimal siAT concentration for ATB gene silencing. siAT concentrations ranging from 65 to 85 pmol were evaluated, and the greatest reduction in ATB mRNA expression was achieved at 65 pmol. To determine the optimal transfection duration, ATB mRNA levels were measured at time points between 12 and 42 h post-transfection at 3-h intervals. The lowest ATB mRNA expression was observed after 16 h of incubation, indicating the maximum gene-silencing efficiency and the strongest inhibitory effect on HepG2 cells.

3.7. siAT-LNP decreases ATB production

Cells were then treated with different formulations containing FITC-labeled siRNA, including naked siRNA-FITC, ligand-conjugated siRNA-FITC, and ligand-conjugated LNP encapsulating siRNA-FITC. All formulations were administered in serum-free medium at a final siRNA concentration of 65 pmol. Following a 4-h incubation period at 37°C, cells were washed twice with ice-cold phosphate-buffered saline (PBS) to eliminate residual extracellular siRNA. Cells were subsequently detached with 0.25% trypsin–EDTA, collected, and centrifuged at 1200 rpm for 5 min at 4°C prior to further analysis.

Cell pellets were reconstituted in ice-cold PBS supplemented with 2% FBS prior to flow cytometric analysis. Flow Cytometry Analysis Fluorescence intensity was measured using a Partec Cyflow flow cytometer (Partec Cyflow, Germany) equipped with a 488 nm excitation laser and a 560 nm emission filter (FITC channel). A total of 1000 events were collected per sample. Unstained cells were included as a negative control for gating purposes. Data were analyzed using FlowJo software (v7.6.1), and uptake efficiency was reported as the percentage of FITC-positive cells (Fig. 9).

3.8. Western blot analysis

The relative expression levels of ATB protein in HepG2 cells treatment with siAT (65 pmol)-LNP exhibited a time-dependent decrease, as shown in Fig. 10. Following normalization to the control groups and β-actin, ATB protein expression was found to be significantly reduced at 48 h post-treatment compared to the 24-h time point. These results demonstrate that treatment with siAT (65 pmol)-LNP leads to a marked suppression of total ATB protein expression in HepG2 cells at 48 h relative to untreated controls.

3.9. Antithrombin chromogenic assay

ATB functional activity was measured in HepG2 cells following treatment with naked siRNA, and two other formulations, including siRNA-LNP and siRNA-LNP-LBN (n = 4). Treatment with naked siRNA did not reduce ATB activity by 86.6 ± 3.1%. siRNA-LNP formulation represented an intermediate reduction in activity, 64.1 ± 2.6%, and siRNA-LNP formulation indicated the largest effect, yielding a marked decrease

in ATB activity, 48.1 ± 5.5%. One-way ANOVA showed a highly significant difference between groups ($p < 0.001$).

4. Conclusion

In the research work, a novel targeted LNP platform that combines a morpholine base as IL (MIL) with a lactobionic (LBN) moiety to achieve efficient, specific delivery of anti-SERPINC1 siRNA to hepatocytes was studied. The optimized siAT-LNP-LBN displayed favorable physicochemical properties, high EE, and low cytotoxicity at therapeutically relevant doses. Decoration with LBN produced markedly increased hepatocyte uptake versus non-targeted LNP and translated into potent ATB mRNA and protein knockdown at optimized dosing and time points. Functionally, this produced the largest reduction in ATB activity compared with the controls, demonstrating that enhanced cellular delivery leads to meaningful anticoagulant modulation. A key advance of this study is the synergistic contribution of both the MIL and the LBN to the overall performance of the targeted formulation. The MIL provides critical and non-immunogenic IL character and endosomal escape capability. Its tailored hydrophobic tail and headgroup chemistry also supported stable particle formation, enabling reproducible manufacture of functional LNP. Complementing the MIL, the LBN ligand furnishes hepatocyte specificity through galactose-mediated recognition of ASGPR, and the octadecylamine anchor ensures stable surface presentation and retention of the targeting moiety on the LNP. MIL maximizes intracellular delivery once internalization occurs, while LBN increases selective uptake by hepatocytes, substantially improving the therapeutic index relative to untargeted particles. These design elements produced a targeted siRNA delivery system that minimizes off-target exposure and potentiates on-target knockdown in hepatocytes, attributes critical for translating ATB-lowering strategies into safe, effective therapies. Moving forward, *in vivo* studies are necessary to characterize the biodistribution, immunogenicity, and safety over acute and chronic dosing. Process optimization and scale-up studies should confirm that the MIL/LBN chemistry is amenable to reproducible manufacturing and stability. Finally, exploration of MIL and LBN modularity varying lipid tail length, headgroup pKa, ligand density, or alternative receptor-targeting glycans could further refine potency and selectivity for diverse hepatocyte-directed siRNA therapeutics. Subsequently, the developed formulation establishes a robust, rationally designed approach for hepatocyte-targeted siRNA delivery [38, 39].

Declarations

Declaration of interests

The authors have no conflicts of interest to declare.

Author Contribution

Conceptualization & Funding acquisition; Y.J., and A.R.Z., Investigation and Methodology; A.R.Z., S.H.K., HR. H., and S.M.S.S.. Project administration; Y.J., Supervision; Y.J., and H.H., Writing-original draft; A.R.Z., and S.H.K., Writing-review and editing; Y.J., HR.H., and H.H.. All of the authors have read and approved the final manuscript.

Acknowledgement

This research article was written as a part of Ph.D. thesis No. 182 for Ali Rajabi Zangi registered at the Faculty of Pharmacy, Tabriz University of Medical Sciences, Iran. The financial aid from the Drug Applied Research Center and Faculty of Pharmacy, Tabriz University of Medical Sciences is greatly acknowledged.

Data Availability

All relevant data supporting the findings of this study are contained within the article

No ethics approval or consent to participate was required for this study

Not applicable for consent for publication

All relevant data supporting the findings of this study are contained within the article

References

1. Mackman N, Tilley RE, Key NS (2007) *Role of the extrinsic pathway of blood coagulation in hemostasis and thrombosis.* Arteriosclerosis, thrombosis, and vascular biology. 27(8):1687–1693
2. Walker C, Royston D (2002) Thrombin generation and its inhibition: a review of the scientific basis and mechanism of action of anticoagulant therapies. Br J Anaesth 88(6):848–863
3. Blanchette VS, Srivastava A (2015) *Definitions in hemophilia: resolved and unresolved issues*. in *Seminars in thrombosis and hemostasis*. Thieme Medical
4. Srivastava A et al (2013) Guidelines for the management of hemophilia. Haemophilia 19(1):e1–e47
5. Tsuchida T et al (2022) Thrombin generation capacity is enhanced by low antithrombin activity and depends on the activity of the related coagulation factors. Thromb J 20(1):29
6. Lu D, Dou F, Gao J (2025) Fitusiran: The first approved siRNA therapy for hemophilia via reducing plasma antithrombin levels, vol 19. Drug discoveries & therapeutics, pp 131–132. 2
7. Pasi KJ et al (2021) Targeting of antithrombin in hemophilia A or B with investigational siRNA therapeutic fitusiran—Results of the phase 1 inhibitor cohort. J Thromb Haemost 19(6):1436–1446
8. Pipe SW et al (2023) Gene therapy with etranacogene dezaparvovec for hemophilia B. N Engl J Med 388(8):706–718

9. Springer AD, Dowdy SF (2018) GalNAc-siRNA conjugates: leading the way for delivery of RNAi therapeutics. Nucleic acid Ther 28(3):109–118
10. Young G et al (2025) Safety and efficacy of a fitusiran antithrombin-based dose regimen in people with hemophilia A or B: the ATLAS-OLE study. Blood 145(25):2966–2977
11. Hu B et al (2020) Therapeutic siRNA: state of the art. Signal Transduct Target Therapy 5(1):101
12. Kiaie SH et al (2025) Antibody targeted delivery of lipid nanoparticles for RNA therapeutics to immune cells. Int J Biol Macromol, : p. 145854
13. Kiaie SH et al (2024) Novel synthesized ionizable lipid for LNP-mediated P2X7siRNA to inhibit migration and induce apoptosis of breast cancer cells. Purinergic Signalling 20(5):533–546
14. Alonso S (2018) Exploiting the bioengineering versatility of lactobionic acid in targeted nanosystems and biomaterials. J Controlled Release 287:216–234
15. Nair JK et al (2014) Multivalent N-acetylgalactosamine-conjugated siRNA localizes in hepatocytes and elicits robust RNAi-mediated gene silencing. J Am Chem Soc 136(49):16958–16961
16. Kumar V et al (2023) *Multivalent Lactobionic Acid and N-Acetylgalactosamine-Conjugated Peptide Nucleic Acids for Efficient In Vivo Targeting of Hepatocytes.* Advanced healthcare materials, 12(12): p. 2202859
17. Nelson BC, Borgos SE (2022) High-throughput synthesis and characterization of next-generation lipid nanoparticles for enhanced in vivo performance. Taylor & Francis, pp 573–576
18. Xu Y et al (2023) Rational design and combinatorial chemistry of ionizable lipids for RNA delivery. J Mater Chem B 11(28):6527–6539
19. Basha G et al (2016) Lipid nanoparticle delivery of siRNA to osteocytes leads to effective silencing of SOST and inhibition of sclerostin in vivo. Mol Therapy Nucleic Acids, 5
20. Brimacombe CA et al (2025) Rational design of lipid nanoparticles for enabling gene therapies, vol 33. Molecular Therapy Methods & Clinical Development, 3
21. Chen S et al (2016) Influence of particle size on the in vivo potency of lipid nanoparticle formulations of siRNA. J Controlled Release 235:236–244
22. Donato MT, Tolosa L, Gómez-Lechón MJ (2014) Culture and functional characterization of human hepatoma HepG2 cells. Protocols in in vitro hepatocyte research. Springer, pp 77–93
23. O'Connell J (2002) *Rt-PCR protocols*
24. Birmingham A et al (2007) A protocol for designing siRNAs with high functionality and specificity. Nat Protoc 2(9):2068–2078
25. Weyermann J, Lochmann D, Zimmer A (2005) A practical note on the use of cytotoxicity assays. Int J Pharm 288(2):369–376
26. Arunachalam K, Sreeja PS (2025) *MTT Assay Protocol*, in *Advanced Cell and Molecular Techniques: Protocols for*. Vitro and In Vivo Studies. Springer, pp 271–276
27. Milstein S et al (2013) *Measuring RNAi knockdown using qPCR*, in *Methods in enzymology*. Elsevier, pp 57–77

28. Wang Q et al (2025) Pulmonary delivery of siRNA anti-TNFα-loaded lipid nanoparticles for rapid recovery in murine acute lung injury. Adv Healthc Mater 14(29):e00695
29. Sule R, Rivera G, Gomes AV (2023) Western blotting (immunoblotting): history, theory, uses, protocol and problems. Biotechniques 75(3):99–114
30. Vayanaperumal K, Vayanaperumal K (2023) Western Blotting a review: Principle, protocol and problem solving. GSC Adv Res Reviews 16(3):178–187
31. Hawley TS, Hawley RG (2024) Flow cytometry protocols, vol 2779. Springer Nature
32. Rees P et al (2022) Imaging flow cytometry. Nat Reviews Methods Primers 2(1):86
33. Bohling SD et al (2012) Comparison of clot-based vs chromogenic factor Xa procoagulant phospholipid activity assays. Am J Clin Pathol 137(2):185–192
34. Moser KA, Funk DM (2014) Chromogenic factor VIII activity assay. Am J Hematol 89(7):781–784
35. Clark AL et al (2015) *Statistical analysis*, in *Does home oxygen therapy (HOT) in addition to standard care reduce disease severity and improve symptoms in people with chronic heart failure? A randomised trial of home oxygen therapy for patients with chronic heart failure*. NIHR Journals Library
36. Movasaghi Z, Rehman S, Rehman DI (2008) *Fourier transform infrared (FTIR) spectroscopy of biological tissues.* Applied Spectroscopy Reviews, 43(2): pp. 134–179
37. Keeler J (2010) Understanding NMR spectroscopy. Wiley
38. Ragni MV, Chan SY (2023) Innovations in RNA therapy for hemophilia. Blood 142(19):1613–1621
39. Shevelev A et al (2025) siRNA Therapeutics for the Treatment of Hereditary Diseases and Other Conditions: A Review. Int J Mol Sci 26(17):8651

Figures

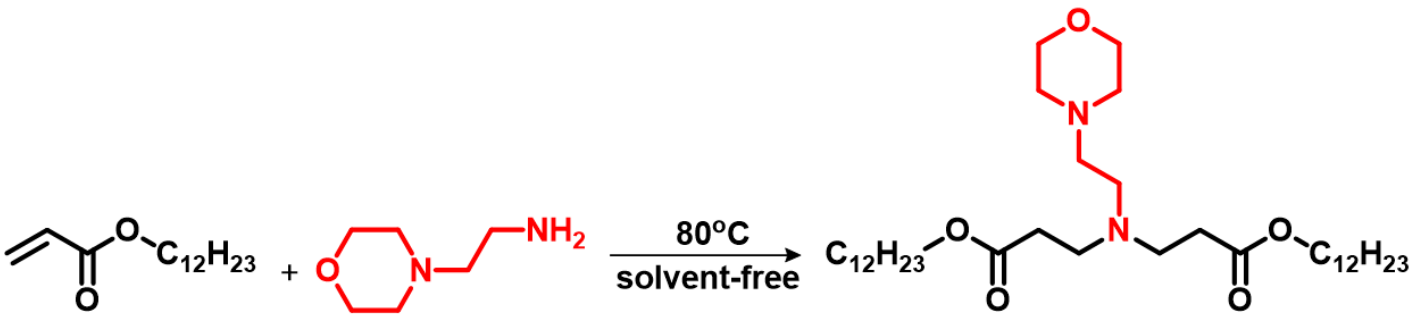


Figure 1

Reaction route of the MIL synthesis.

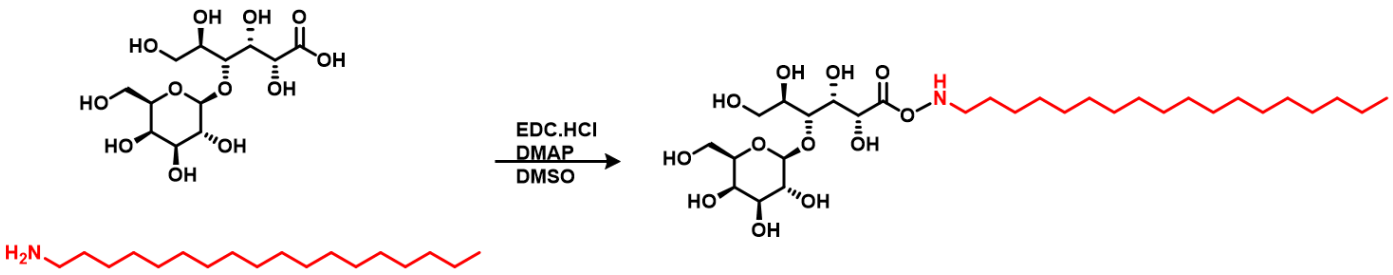


Figure 2

Reaction route of the LBN synthesis.

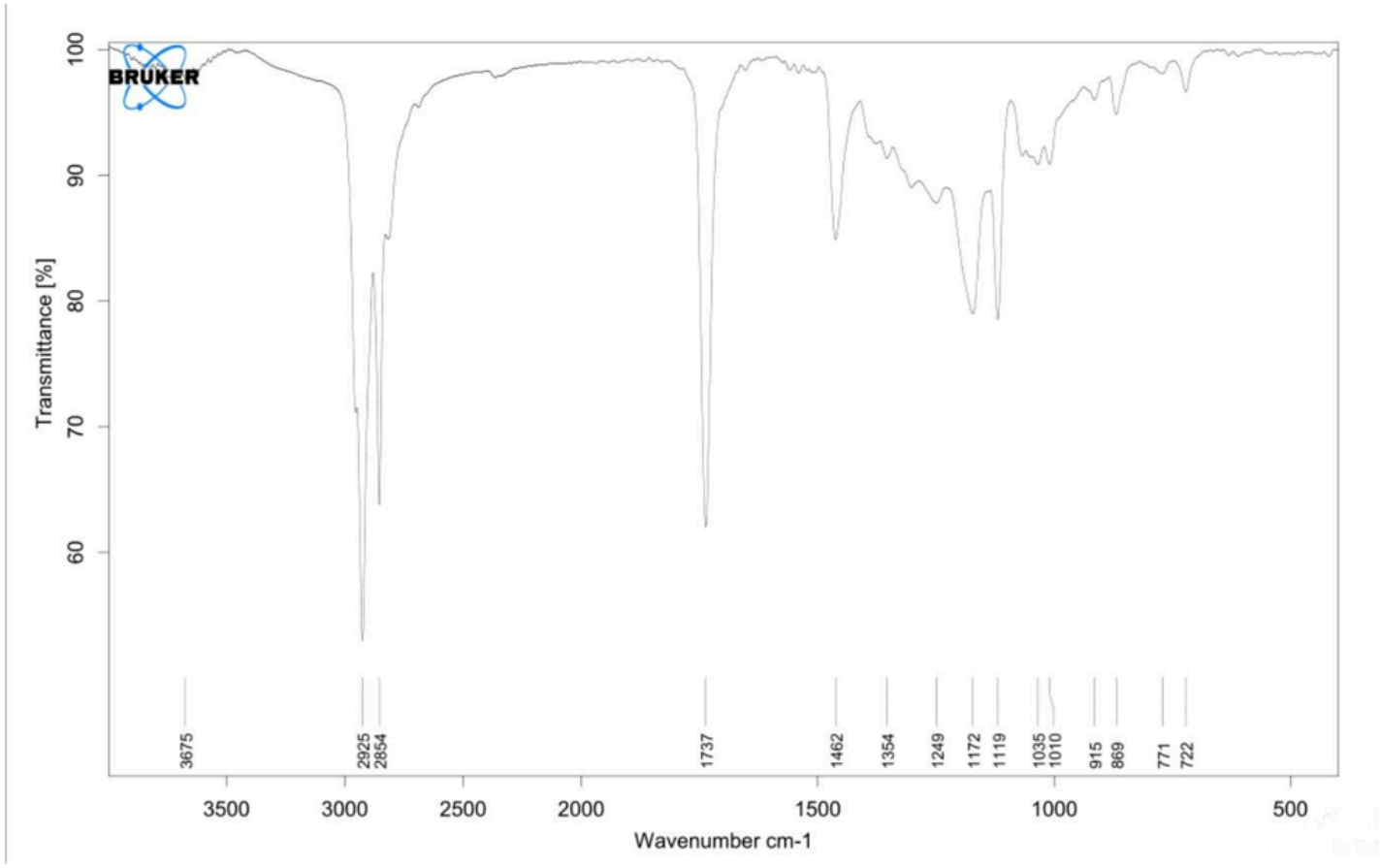


Figure 3

FT-IR spectrum interpretation of MIL .

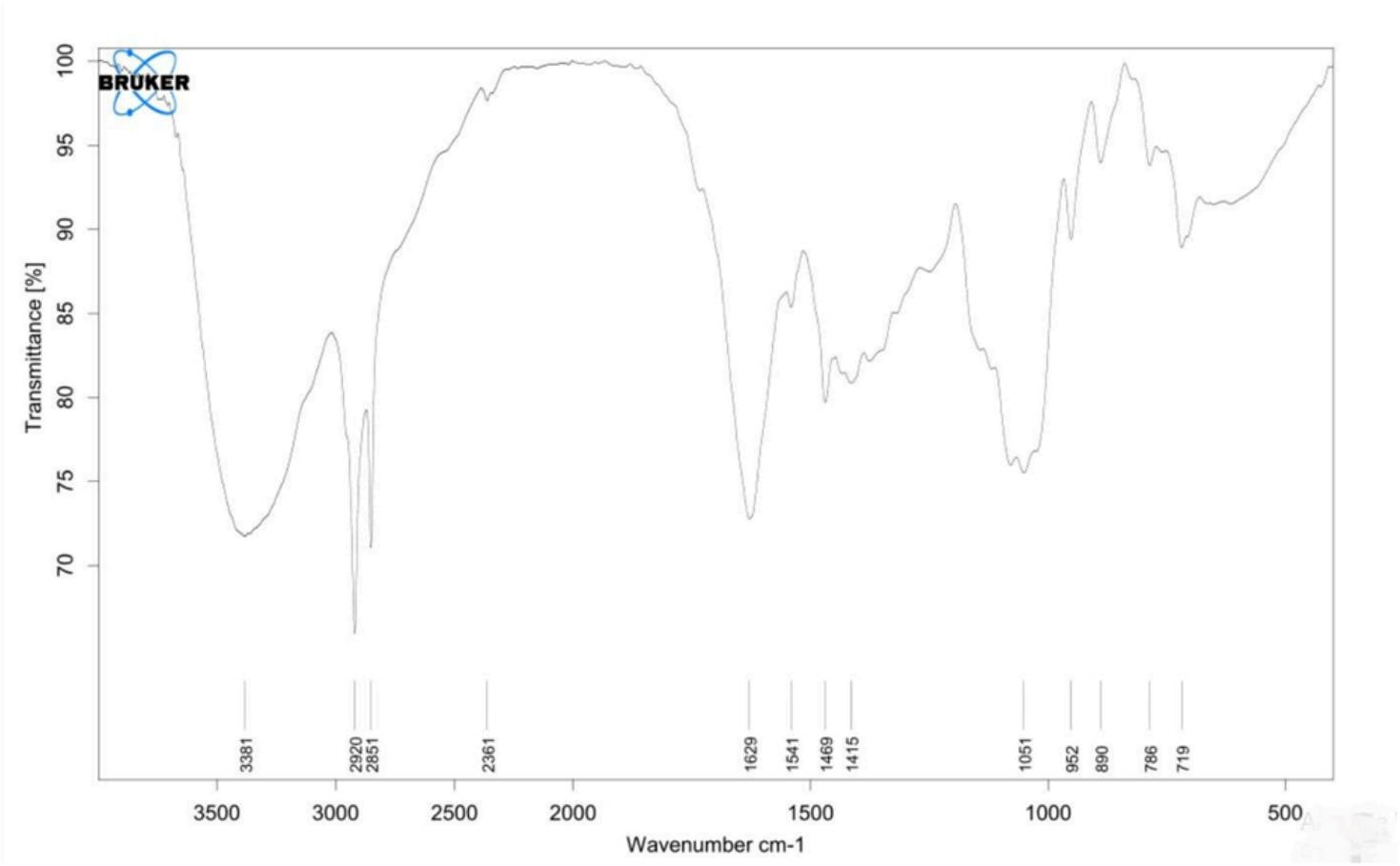


Figure 4

FT-IR spectrum interpretation of LBN.

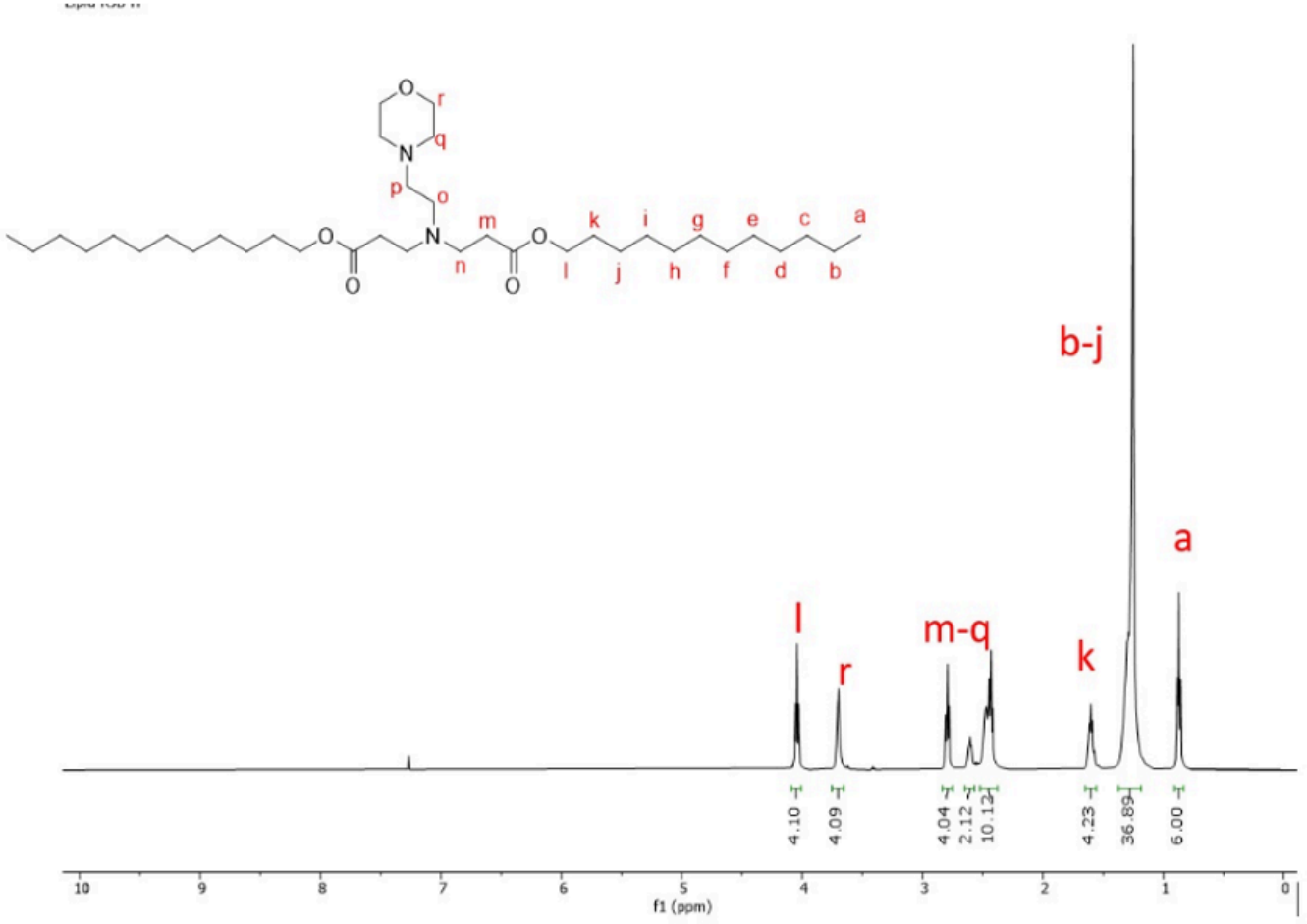


Figure 5

The assignment of ^{1}H-NMR spectra for MIL.

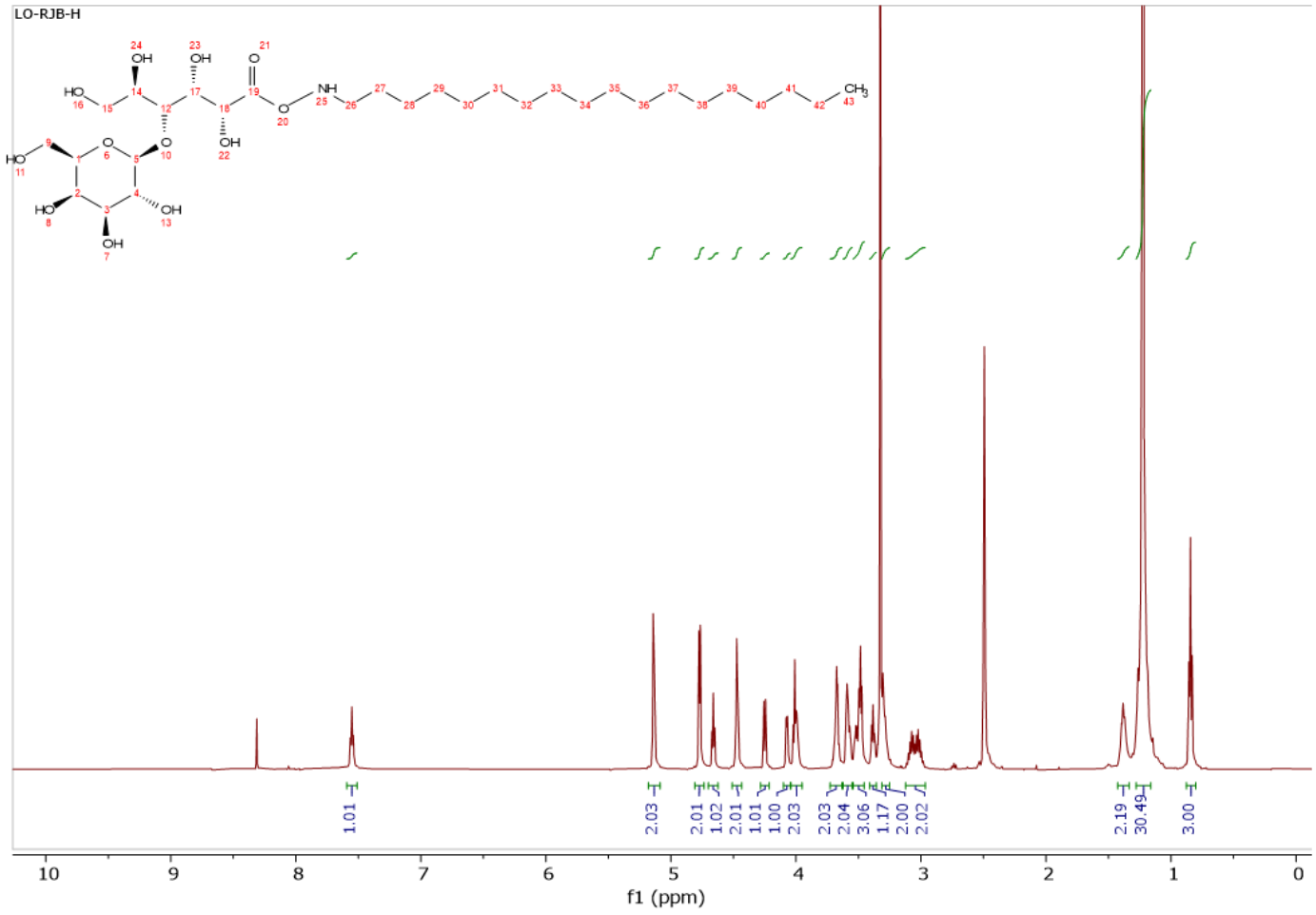
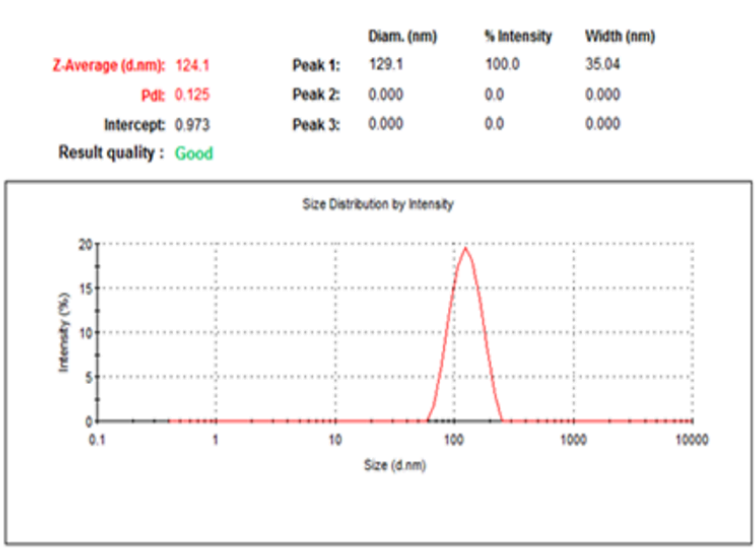


Figure 6

The assignment of ^{1}H-NMR spectra for LBN.



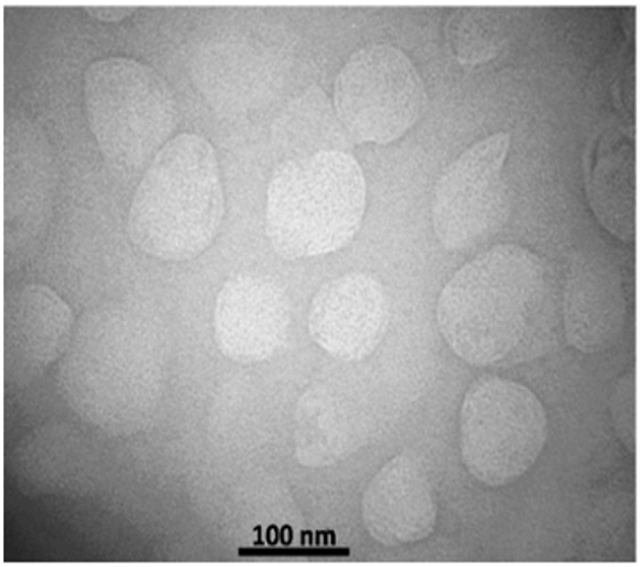


Figure 7

Characterization, Left) DLS results and Right)TEM image of siAT-LNP-LBN.

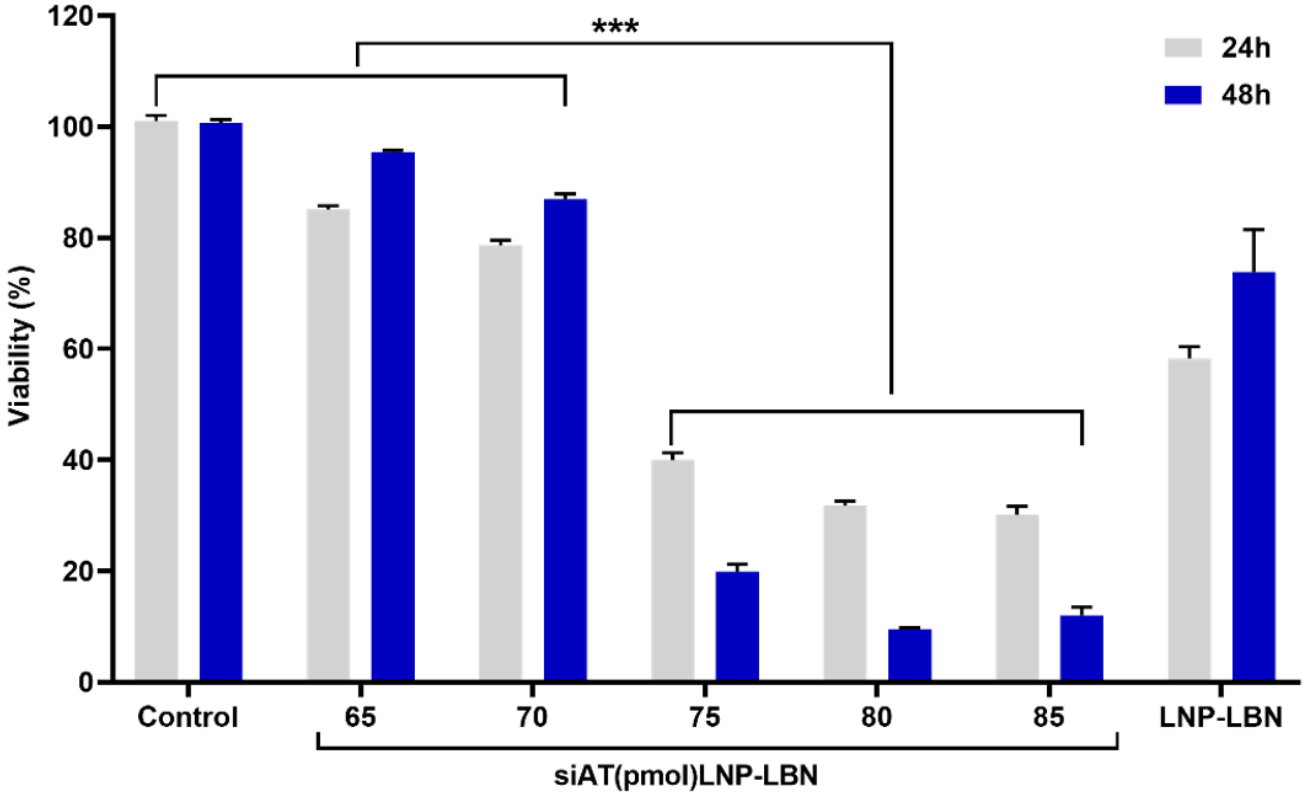


Figure 8

Evaluation of HepG2 cell viability for treated different siAT concentrations (65-85 pmol) in siAT-LNP-LBN formulations compared with the control after 24 and 48 h of incubation (*** p values < 0.001).

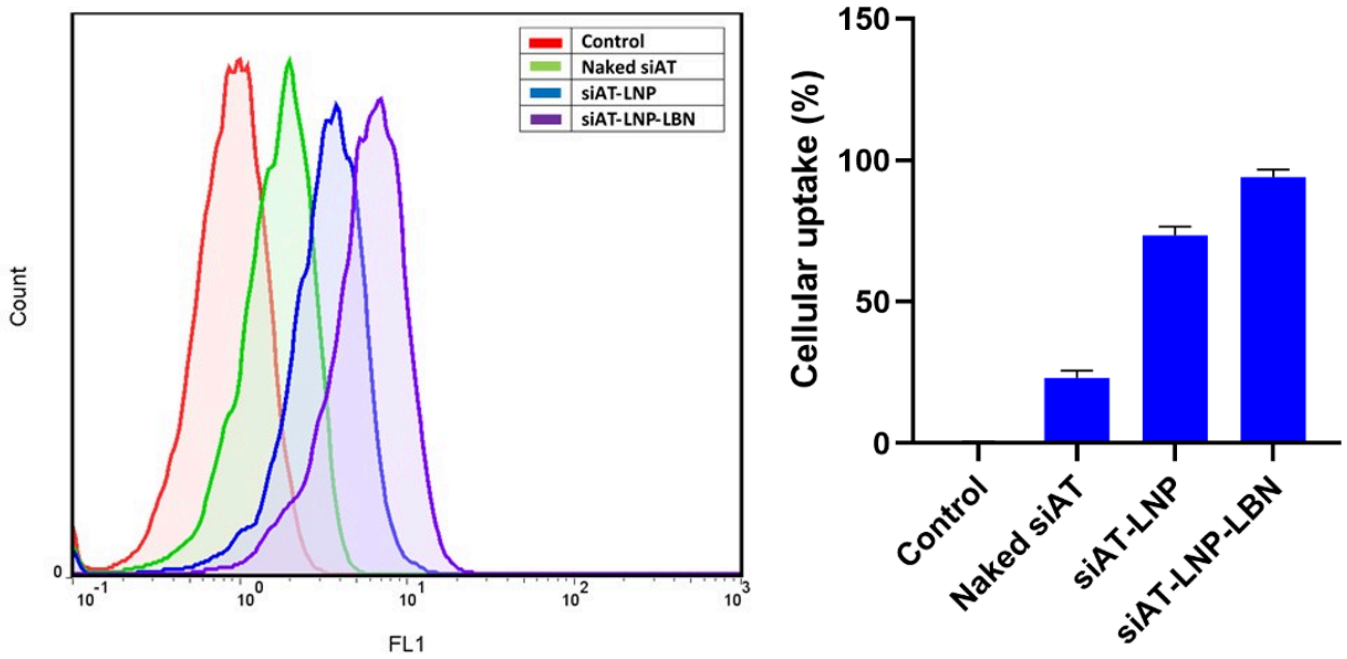


Figure 9

HepG2 Cell uptake using flowcytometry for Control, Naked siAT, siAT-LNP, and siAT-LNP-LBN.

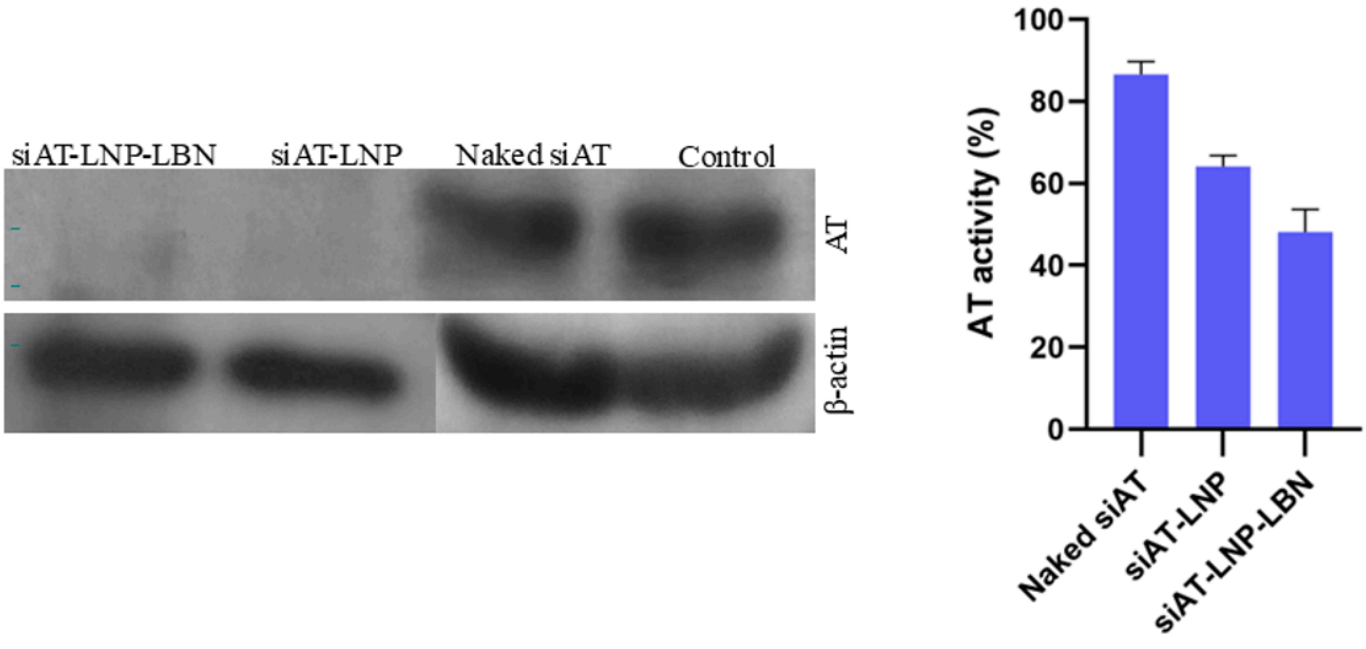


Figure 10

Left; ATB protein expression and functional activity following siAT-mediated gene silencing in HepG2 cells. (A) Representative Western blot analysis of ATB and β-actin protein expression in HepG2 cells treated with siAT-loaded LNPs (65 pmol) for 48 h. (B) Densitometric quantification of ATB protein levels

relative to the control group. Data are expressed as mean ± SD of three independent biological replicates (**p < 0.01, ***p < 0.001). (C) Functional assessment of ATB activity by the heparin cofactor activity assay following transfection with naked siAT, siAT-LNP, and siAT-LBN-LNP formulations